Proceedings of the
International Conference on Mechanical Engineering 2005
(ICME2005) 28 - 30 December 2005, Dhaka, Bangladesh

ICME05-FL-09

DRAG MEASUREMENTS OF A RUGBY BALL USING EFD AND CFD

Firoz Alam, **Pek Chee We, Simon Watkins and Aleksandar Subic**

School of Aerospace, Mechanical and Manufacturing Engineering, RMIT University
264 Plenty Road, Bundoora, Melbourne, VIC 3083, Australia

ABSTRACT

The aerodynamic drag, side and lift forces of a rugby under a range of yaw angles were measured both experimentally in wind tunnel and computationally using computational fluid dynamics method and compared with experimental findings. Flow visualization around the ball was conducted with wool tufts and smoke and illustrated the complexity of the flow structure. The average drag coefficient of the rugby at zero yaw was found by experimentally and computationally to be 0.18 and 0.15 and this rose to about 0.60 and 0.31when yawed at 90 degrees respectively. There was minor Reynolds number sensitivity at zero yaw but this was more significant at yaw angles of around 90 degrees in experimental results. However, these sensitivities were not found in computational results.

Keywords: Drag, Side Force, Wind Tunnel, Experimental Fluid Dynamics, Computational Fluid Dynamics.

1. INTRODUCTION

Airflow around a sporting ball plays a significant role as it influences the speed, motion, trajectory and ultimately place of landing of the ball. Despite the popularity of games such as Rugby[1], there appears to be scant aerodynamic research in the area. In the recent World Rugby Cup it was clearly evident that distance kicking plays an increasingly significant role in the outcome of the game thus a study into the aerodynamics forces seems timely.

Prior aerodynamic studies on spherical sporting balls [2], [3] and [4]. However, no knowledge about the aerodynamic forces of more "ellipsoidal" balls is available in the public domain. Therefore, the primary objective of this study was to investigate the steady-state aerodynamic properties, such as drag and side force (or lift) of a rugby ball. Ultimately the work will be extended to understanding the complexities of spinning balls but here it is restricted to non-spinning flight. The experimental study was conducted at RMIT Industrial Wind Tunnel using a six component force sensor (for details see, [1 & 2]). The computational study was also done on rugby ball using commercial software Fluent.

2. EXPERIMENTAL MEASUREMENTS AND EQUIPMENT

New Rugby ball made by SUMMIT Australia has been selected for this work as it is officially used in various tournaments in Australia. The dimensions of the Rugby ball used for this work were 280 mm in length and 184 mm in diameter. The ball was made of four synthetic rubber segments (see Figures 1 and 2 a & b). It should be noted that the Rugby is closely circular in section and fatter compared to American and Australian Rules football. A sting mount was designed to hold the ball, see Figures 1 & 2. Figures 1 shows the experimental set up in the wind-tunnel test section. The distance between the bottom edge of the ball and the tunnel floor was 350 mm, which is well above the tunnel's boundary layer and considered to be out of significant ground effect.

Fig 1. Rugby ball in RMIT wind tunnel

[1] Rugby is played in over 100 countries.

a) Rugby ball (side view)

b) Rugby ball (longitudinal view)

Fig 2. Rugby ball on force sensor in wind tunnel

3. CFD MODELLING PROCEDURES

A simplified (smooth oval shape) rugby ball was constructed in GAMBIT. The centre or the heart of the rugby ball is located at the origin of the 3 axis. The length of the rugby ball is along the Z-axis with 0.28 units and the height 0.184 units along the Y-axis. After the vertices were marked as the dimensions of the rugby ball, the first half of the rugby ball was drawn. For this part, the vertices were connected by drawing edges across them. The edges defined the geometry and shape of the rugby ball. The second half was drawn by flipping the geometry in 360 degrees to generate an oval volume. The next step was to draw the overall wind tunnel test section dimensions shown in Figure 3. After the model drawn, face was created for the model. As the model is a 3 dimensional, 6 faces are required for the wind tunnel and 1 face for the ellipsoidal rugby ball. In order to create a face, it was necessary for all the edges to be connected to each other. An opened side will disallow the creation of a face. When the face is successfully created, the edges will turn blue from yellow colour. The next step was to create the volume. The created volume of the rugby ball is shown in Figure 4. The volume of the rugby ball was created by revolving the face by a 360 degrees rotation with the Z-axis line edge as the centre. For the wind tunnel, it was simply done by stitching all the 6 faces of the rectangular geometry. After the creation of the volume for the wind tunnel, the volume of the wind tunnel was subtracted by the volume of the rugby ball as the rugby ball is solid and the area within the wind tunnel is empty. The next step was to mesh the whole model as shown in Figures 5 & 6. At first, the meshing of the faces was required. The meshing of the rugby ball and the wind tunnel faces was used with Tri mesh. As the ball is a 3D and ellipsoidal shaped geometry, Tri meshing is more suitable compared to Quad meshing. After well meshing the faces of the wind tunnel, the final volume of the model was meshed using Tet/Hybrid mesh. The specifications of the meshing are: rugby ball face using Tri mesh of interval size of 0.02, wind tunnel faces using Tri mesh of interval size of 0.1, and whole volume mesh using Tet/Hybrid mesh of interval size 0.1. The finished meshed model is shown in Figure 6. The finished mesh can be refined further in FLUENT software if requires.

The boundary conditions for the modelling were: the frontal area of the wind tunnel was the velocity inlet as the wind source comes from there and the rear face area of the wind tunnel was the pressure outlet as the wind exits the test section from there. The rest of the boundary types were specified as walls including the rugby ball, which is also considered as wall.

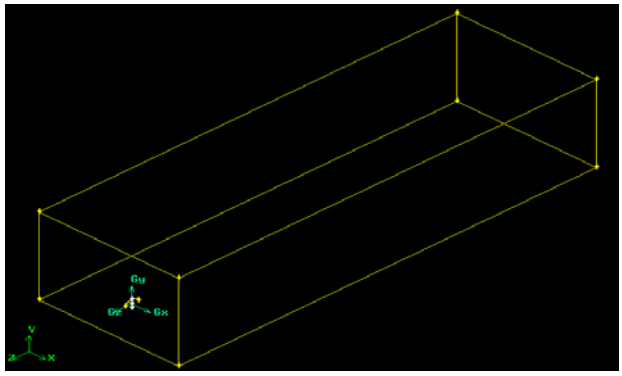

Fig 3. Wind Tunnel Test Section in CFD

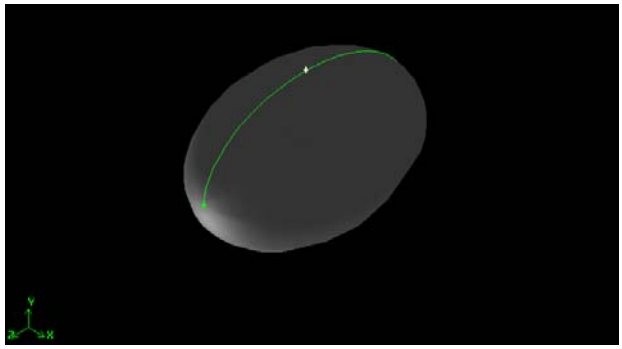

Fig 4. Volume of the Rugby Ball in CFD

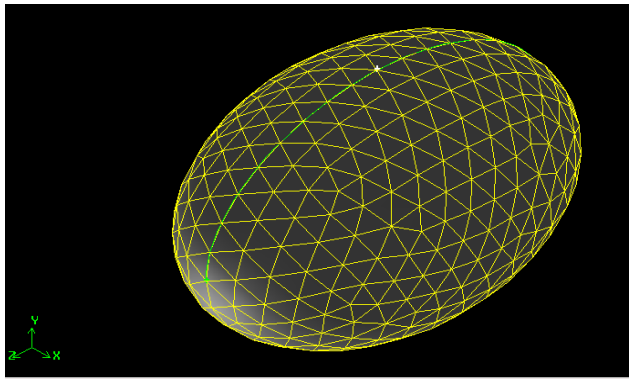

Fig 5. Meshing of the Rugby Ball in CFD

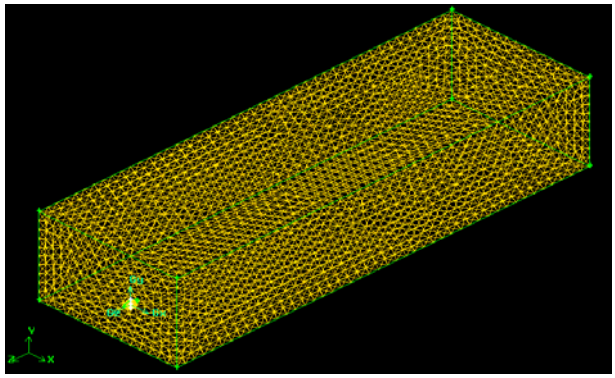

Fig 6. Wind Tunnel Meshing in CFD

3.1 Fluent Analysis Procedure

The GAMBIT model was imported to Fluent and the grid was checked to eliminate any errors in the model before starting the simulation. The Segregated (Implicit) solver was selected for the computation as it is faster and produced results close to experimental findings. Additionally, the segregated implicit solver is widely used for incompressible and mildly compressible flows. The flow was defined as inviscid, laminar and/or turbulent and the k-epsilon model was selected for the turbulence modelling. The non-equilibrium wall function was used as the flow is complex involving separation, re-attachment and impingement. Under boundary conditions, the various flow parameters were specified such as the wind speed, turbulence etc. The direction of airflow was normal to the inlet and the reference frame was set as absolute for the velocity. In order to control the solution, the 2nd order upwind scheme interpolation was selected as the simulation involves Tri/tetrahedral meshes. After setting all corresponding parameters, the simulation was initialized and iterated, and the results were obtained.

4. RESULTS AND DISCUSSION

4.1 Experimental Results

The Rugby ball was tested in wind tunnel at 60, 80, 100, 120 and 140 km/h speeds under +100° to -80° yaw angles with an increment of 10°. Wool tufts and smoke were used to visualise the flow around the ball at various yaw angles. The ball was yawed relative to the force balance (which was fixed with its resolving axis along the mean flow direction whilst a ball was yawed above it) thus the wind axis system was employed. Flow visualisation by wool tufts at 0° and 90° yaw angles are shown in this paper (see Figure 7). The forces and moments were converted to non-dimensional parameters and tare forces were removed by measuring the forces on the sting in isolation and them removing them from the force of the ball and sting. Only drag force coefficients are presented in this work and they are plotted against yaw angles. Figure 8 shows the drag coefficient variation with velocities and yaw angles for the Rugby ball.

a) Flow Pattern at 0º Yaw b) Flow Pattern at 90º yaw

Fig 7. Flow Structure around a Rugby Ball

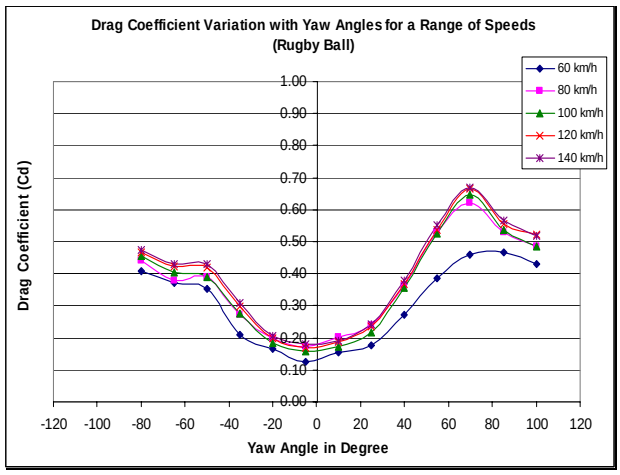

Fig 8. Drag Coefficients as a Function of Yaw Angles and Speeds

A comparison of drag coefficients at all speeds and yaw angles for the Rugby Ball indicates that there is a slight lack of symmetry in the results (Figure 8). Whilst some errors arose from a slight lack of airflow and force balance symmetry, the errors are greater than expected. Examination of the ball indicated that the ball is not exactly symmetrical. The average drag coefficient of the Rugby ball was experimentally found to be 0.18 at zero yaw angle. No significant variation in Reynolds numbers was evident at 90° yaw angle for the Rugby ball except for the 60 km/h speed (see Figure 8). With an increase in yaw angle, the drag coefficient increases due to a large and very complex flow separation. Flow visualisation was conducted at 60, 100 and 140 km/h under ±90° yaw angles with an increment of 10° but is only given here for 60 km/h. Flow structures at 90° are complex. Flow separations start at approximately ¾ length from the front edge at zero yaw angles for both types of ball and the separations are complicated and time varying at 90° yaw angle.

4.2 Computational Results

The computational simulation was conducted using Fluent 6.1 at a range of speeds (60 to 120 km/h with an increment of 20 km/h). The velocity vectors and static pressure distributions around the ball at 0 and 90 yaw angles for 100 km/h speed are shown in Figures 9 to 12. The drag coefficients (Cd) for 60 to 120 km/h with an increment of 20 km/h at ±90º yaw angles are shown in Figure 13. A significant variation in velocity vectors between 0º and 90º yaw angles is evident (see Figures 9 and 10). At 0º yaw angle. The flow is more streamlined and attached compared to 90º yaw angle as expected. The velocity vectors are more chaotic in the leeward side of the ball (behind) at 90º compared to 0º yaw angle where the velocity vectors are relatively streamlined to the mean direction of the flow. The static pressure distribution pattern has similar trend like sphere. The highest negative pressure is noted at the lateral side at 90º yaw angle compared to 0º yaw angle (see Figures 11 & 12). However, a close inspection indicates that the pressure distributions are absolutely not symmetrical around the ball. As mentioned earlier, the drag

coefficient distribution as a function of yaw angles and speeds is shown in Figure 13. No Reynolds number variation is found in CFD analysis. The drag coefficients are independent of Reynolds numbers. The computed minimum drag coefficient at ±15º (including 0º) yaw angles was approximately 0.15. However, the drag coefficient increases with an increase of yaw angles (see Figure 13). The maximum drag coefficient was found at ±90º yaw angles (approximately 0.31). No significant asymmetry of drag coefficients between the positive and negative yaw angles was noted.

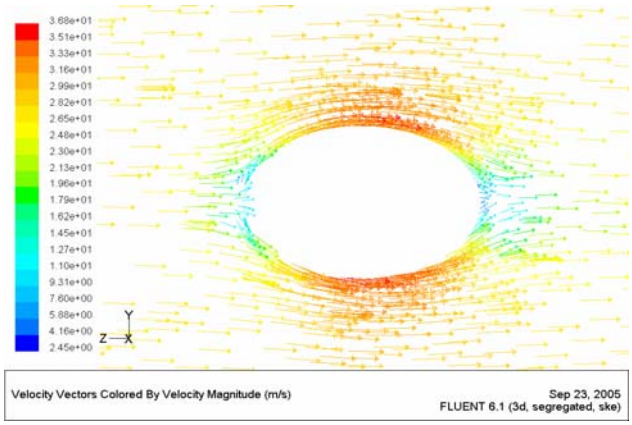

Fig 9. Velocity vectors around the rugby ball at 0º yaw

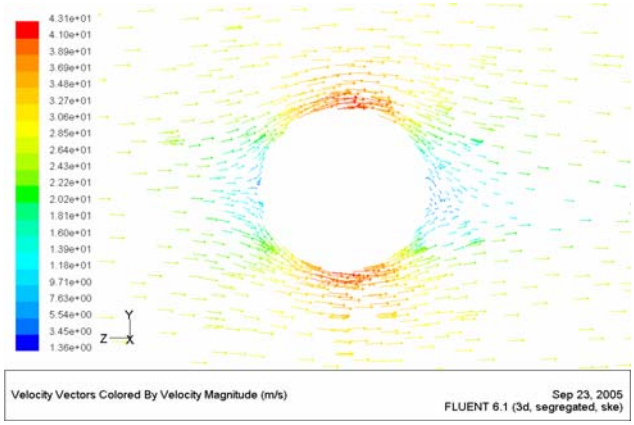

Fig 10. Velocity vectors around the rugby ball at 90º yaw

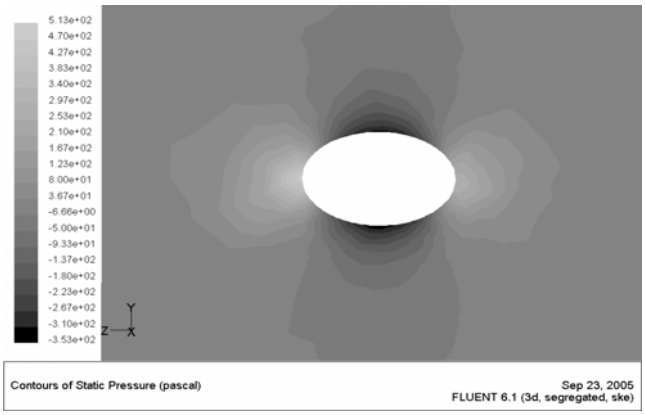

Fig 11. Static Pressure Distribution around the rugby ball at 0º yaw

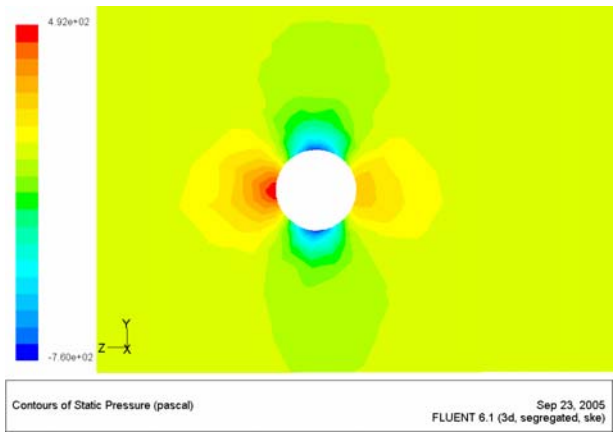

Fig 12. Static Pressure Distribution around the rugby ball at 90º yaw

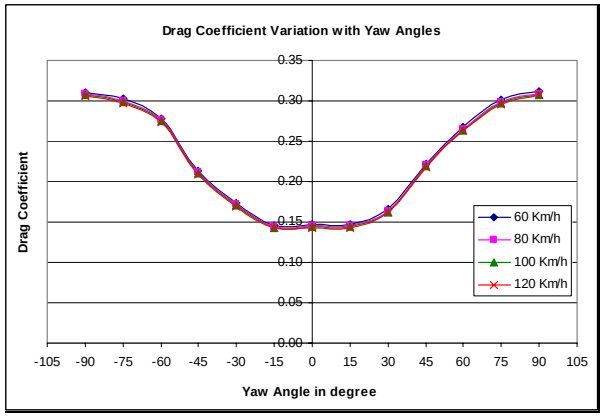

Fig 13. Drag Coefficients as a Function of Yaw Angles

4.3 General Discussion

The flow visualisation (with wool tuft and smoke) around the Rugby ball indicated complex flow structures at 90 yaw angles. The similar flow pattern but lesser extent was also noted at 0 yaw angle. The separation was three dimensional in the leeward side of the ball. The experimentally determined drag coefficient (0.18 at 0 yaw angle and 0.6 at 90 yaw angle) is higher compared to computationally estimated drag coefficient (0.15 at 0 yaw angle and 0.31 at 90 yaw angle). The Reynolds number dependency was noted at 90 yaw angle in experimental analysis. However, no Reynolds number dependency was noted in computational analysis. A close inspection has revealed that the Rugby ball is not fully symmetrical along the longitudinal axis. The ball surface was rough and was not fully oval shape as it was made of four segments. On the other hand, the Rugby ball in CFD analysis was fully symmetrical along the longitudinal and lateral axes. The surface was smooth and the flow was uniform. The cross sectional area was fully circular compared to the real rugby ball. Visual inspection has revealed that the cross sectional geometry is slightly larger compared to a circular geometry that modelled in CFD.

The geometry of a real Rugby ball is complex as a parabolic 3D shaped ball is hard to manufacture to perfection. Due to this factor, the rugby ball is not symmetrical in reality as mentioned earlier. However, in

CFD, modelling of a perfectly symmetrical parabolic geometry is simple. On the other hand, in CFD, it is difficult to model the cross sectional geometry to the exact rugby ball shape, hence the rugby ball modelled in CFD was constructed generally to a perfect circle for the cross section. Using CFD, ideal theoretical results were generated. However, in reality, the experimental approach is more realistic as it incorporates the real flow. The accuracy in experimental results may be compromised due to some external factors and errors.

5. CONCLUSIONS

- The aerodynamics resulting from the flight of irregular shaped sporting balls is extremely complex even when the ball is not spinning.
- The average drag coefficient for the rugby ball at zero yaw angles was found experimentally and computationally to be 0.18 and 0.15 respectively.
- The experimental and computational measurements indicated the average drag coefficient for the rugby ball at 90º yaw angles between 0.60 and 0.31.
- No Reynolds number variation of drag coefficients was found in computational analysis. However, some variations were noted in experimental measurements.

6. RECOMMENDATIONS FOR FURTHER WORK

The following recommendations for future works can be made:

- Effects of spin on aerodynamic drag, lift and side force
- Compare the drag coefficients for three major manufacturers' balls: Summit, Adidas and Gilbert

7. ACKNOWLEDGEMENT

The authors would like to express their sincere gratitude to Mr Greg McLyntyre, SUMMIT Australia for providing the Rugby balls.

8. REFERENCES

1. Alam, F., Subic, A. and Watkins, S., 2005, "Measurements of aerodynamic drag forces of a rugby ball and Australian Rules football", *Proc. Asia Pacific Congress on Sports Technology (APCST2005)*, pp. 276-279, Tokyo Institute of Technology, 11-14 September, Tokyo, Japan.
2. Alam, F., Watkins, S. and Subic, A., 2004, "The Aerodynamic Drag of a Rugby Ball and Australian Rules Foot Ball", *Proc. of the 5th Bluff Body Aerodynamics and Applications (BBAA V) Conference,* pp. 211-214, 11-15 July, Ottawa, Canada.
3. Cooke, A. J., 2000, "An overview of tennis ball aerodynamics", *Sports Engineering*, **3** (2), pp. 123-129.
4. Mehta, R. D. and Pallis, J. M., 2001, "The aerodynamics of a tennis ball", *Sports Engineering*, **4** (4), pp. 1-13.

9. NOMENCLATURE

Symbol	Meaning	Unit
Cd	Drag coefficient	(-)
Ψ	Yaw angle	(º)
P	Pressure	(Pa)